Chemical Engineering Science, Vol. 47, No. 13/14, pp. 3265–3272, 1992.
Printed in Great Britain.

0009–2509/92 $5.00+0.00

PREDICTION OF THE BUBBLE SIZE GENERATED BY A PLUNGING LIQUID JET BUBBLE COLUMN

G.M. Evans, G.J. Jameson and B.W. Atkinson

Department of Chemical Engineering,
University of Newcastle, N.S.W., 2308, Australia

ABSTRACT

In this paper a model is presented to predict the maximum bubble size generated within the mixing zone at the top of a plunging liquid jet bubble column. The model uses a critical Weber number, where the energy dissipation rate per unit volume is derived from the theory of liquid-jet gas ejectors. The length of the mixing zone, and hence its volume, was determined experimentally from the vertical axial pressure profile along the wall of the column. The model was tested experimentally for a range of column and jet diameters, jet velocities, and liquid physical properties, and it was found that the measured maximum bubble diameter was in good agreement with the model predictions based on a critical Weber number of 1.2. It was also found that the bubble diameter distribution was fitted by a log-normal distribution, with a Sauter-mean-to-maximum-diameter ratio of 0.61 which is consistent with reported literature values.

KEYWORDS

Plunging liquid jet, Downflow bubble column, Bubble diameter, Weber number

INTRODUCTION

Figure 1 shows a schematic of a plunging liquid jet bubble column where both the gas and liquid are introduced at the top of the reactor. The liquid feed is in the form of a high velocity jet which passes through the headspace at the top of the column and entrains gas as it plunges into the liquid. A region of high recirculation and energy dissipation, known as the mixing zone, is generated at the top of the column where the entrained gas is broken into fine bubbles before being transported downward by the liquid flow, and discharged through the opening at the base of the column.

The size of bubbles produced within the mixing zone is determined by the forces acting on the bubble. In low viscosity liquids the bubbles are deformed by forces arising from liquid velocity fluctuations acting over distances of the order of the bubble diameter, d. The restoring force resisting the deformation of the bubble is due to surface tension acting at the gas-liquid interface. The ratio of these two forces is known as the Weber number, and can be written as $We = \rho\overline{u^2}d/\sigma$, where $\overline{u^2}$ is the average value of the squares of the velocity differences, and σ and ρ are surface tension and liquid density respectively.

The Weber number can be used to predict a maximum stable bubble diameter d_m, by assuming that a bubble will split once a critical Weber number, We_c, is reached, i.e.

$$We_c = \frac{\rho\overline{u^2}d_m}{\sigma} \tag{1}$$

where $\overline{u^2}$, in this case, is the average value of the squares of the velocity differences acting over a length scale equivalent to the maximum bubble diameter d_m.

In this paper the critical Weber number is related to the average energy dissipation rate per unit volume within the liquid to predict the maximum bubble diameter within the mixing zone at the top of a plunging liquid jet bubble column. The effects of jet and column diameter, jet velocity, and liquid physical properties on the resultant bubble size are measured and compared with the model predictions.

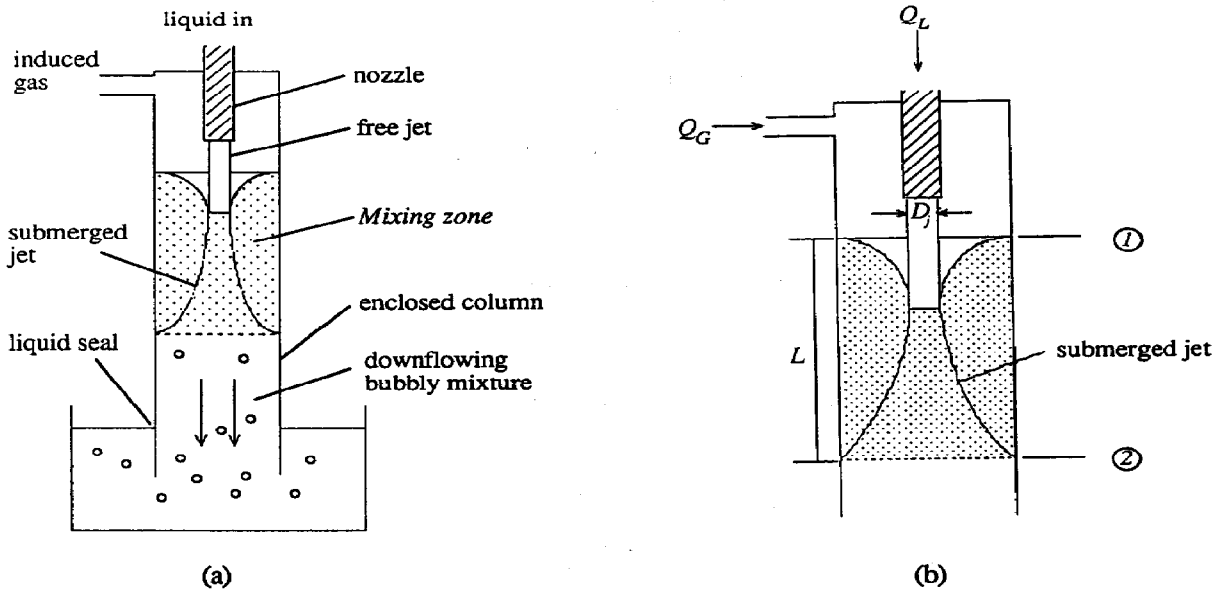

Fig. 1. Plunging liquid jet bubble column.

THEORETICAL

The maximum stable bubble diameter can be calculated from eq. (1) provided the liquid physical properties, critical Weber number, and average of the squares of the velocity fluctuations acting over length scales of the same order as the bubble diameter are known.

If the bubble is small compared to the turbulent macroscale but large compared to the microscale, the eddies responsible for breakup are isotropic and lie within the inertial subrange such that their kinetic energy is independent of viscosity and follows the Kolmogoroff energy distribution law, i.e.

$$\overline{u^2} = C_1\left(\frac{\varepsilon d}{\rho}\right)^{2/3} , \tag{2}$$

where ε is the average energy dissipation rate per unit volume, and the constant $C_1 \approx 2.0$ according to Batchelor (1951). Substituting this expression into eq. (1), and rearranging, results in an expression for the maximum stable bubble diameter:

$$d_m = \left(\frac{We_c\sigma}{2}\right)^{3/5}(\rho)^{-1/5}(\varepsilon)^{-2/5} . \tag{3}$$

Equation (3) has been derived assuming that the average energy dissipation rate per unit volume experienced by the bubble is uniform throughout the field. For flows where the energy dissipation rate per unit volume is not uniform throughout the field, such as in the mixing zone of a plunging liquid jet bubble column, the energy dissipation rate which determines the maximum bubble diameter for the entire flow field should be used.

The energy dissipation rate that determines the maximum bubble size in the mixing zone can be found by considering what happens to the entrained gas. Initially, all of the entrained gas enters the mixing zone at the plunge point of the liquid jet. The high energy dissipation in this region results in the generation of a number of very fine bubbles which are carried downward by the bulk liquid motion and leave the mixing zone. However, a number of larger bubbles are also generated, which recirculate within the mixing zone where they are eventually broken up and carried downward by the bulk liquid flow. Order of magnitude calculations based on the rise velocity of the bubble and the downward superficial liquid velocity, show that the residence time of the larger bubbles inside the mixing zone is of the order of one second, and this would allow a sufficient number of breakages to occur so that an equilibrium maximum stable bubble is reached. Furthermore, according to Hinze (1955), if the flow field is not too inhomogeneous, the powerful

diffusive action of turbulence causes the average size of the largest bubble in the whole field to correspond to the average energy dissipation rate across this field.

The average energy dissipation rate per unit volume within the mixing zone of a plunging liquid jet bubble column can be calculated from an energy balance across the mixing zone volume. Following the analysis of Cunningham (1974) for a liquid jet gas pump, and realising that the mixing zone corresponds to the throat section of such a pump, the specific energy dissipation, e_s, within the mixing zone is given by

$$e_s = \frac{u_j^2}{2}\left[1-2b-b^2(1+\gamma\lambda_1)(1+\lambda_2)^2+2b^2(1+\gamma\lambda_1)(1+\lambda_2) - \frac{2\gamma\lambda_1 b^2}{1-b}+\gamma\lambda_1^3\frac{b^2}{(1-b)^2}\right] - \frac{\lambda_1 P_1}{\rho}\ln\frac{P_2}{P_1} \quad , \tag{4}$$

where ρ is the liquid density; u_j is the jet velocity; γ is the gas/liquid density ratio, λ is the gas/liquid volumetric flow ratio; b is the jet/column area ratio; P is the absolute pressure; and the subscripts 1 and 2 refer to the inlet and outlet respectively of the mixing zone (see Fig. 1b).

Equation (4) can be simplified by assuming (i) that $\gamma = 0$, and (ii) that the change in pressure across the mixing zone is negligible, i.e. $P_1 = P_2$. This assumption is based on measurements by Evans (1990) who found that the work associated with compressing the gas within the mixing zone accounted for approximately one percent of the total work received by the gas. From the above-mentioned assumptions $\lambda_1 \approx \lambda_2$, which leads to

$$e_s \approx \frac{u_j^2}{2}\left[1-2b-b^2(1+\lambda_1)^2+2b^2(1+\lambda_1)\right] \quad . \tag{5}$$

The energy dissipation rate per unit volume is obtained by multiplying eq. (5) by the jet mass flow rate, $(\rho u_j \pi D_j^2/4)$, and dividing by the mixing zone volume, $(\pi D_c^2 L/4)$, where D_c is the column diameter and L is the length of the mixing zone (see Fig. 1b). This leads to

$$\varepsilon \approx \frac{\rho u_j^3}{2L}\left[b-2b^2-b^3(1+\lambda_1)^2+2b^3(1+\lambda_1)\right] \quad . \tag{6}$$

Equation (6) can be used in conjunction with eq. (3) to predict the maximum stable bubble diameter, providing the length of the mixing zone and the critical Weber number are known.

At present there is no theoretical model available that can predict the expansion of a submerged bubbly jet within a confined volume. Therefore, the length of the mixing zone is best determined experimentally.

A critical Weber number can be chosen from a number of theoretical and numerical studies relating to the breakup of bubbles. Thus Hinze (1955) gives a value of 1.18 based on the breakup of a droplet or bubble in a viscous shear flow; Sevik and Park (1973) give a value of 1.24 based on the assumption that a bubble will oscillate violently and break up when the characteristic frequency of the turbulence is equal to one of the resonant frequencies of the bubble; Miksis *et al.* (1981) predicted a value of 3.23 for a bubble in a uniform flow; Lewis and Davidson (1982) found that a cylindrical bubble became unstable in an axisymmetric inviscid shear flow at a critical Weber number of 4.7; Ryskin and Leal (1984) predicted that the critical Weber number was a function of the Reynolds number and gave values in the range 0.95 – 2.76 for a bubble in a uni-axial extensional Newtonian flow.

Alternatively, bubble diameter measurements can be used to determine the appropriate critical Weber number for the mixing zone of a plunging liquid jet bubble column.

EXPERIMENTAL

Apparatus

A general layout of the experimental apparatus is given in Fig. 2(a). It consisted of a vertically positioned perspex column with its base extending 25mm below the surface of a constant level bath. Three columns were used in the study and their inside diameter measurements were 44, 74 and 95mm respectively. All three columns were identical in design, constructed from clear perspex, and consisted of a flanged section at

the top which was bolted to the lower part of the chamber at the top of the bubble column. Below the flange was a straight length of clear perspex tube of length 1040mm. The top of the column was sealed from the atmosphere allowing air to pass into the column only through an inlet at the top. The air flow rate into the column was measured using a network of calibrated rotameters.

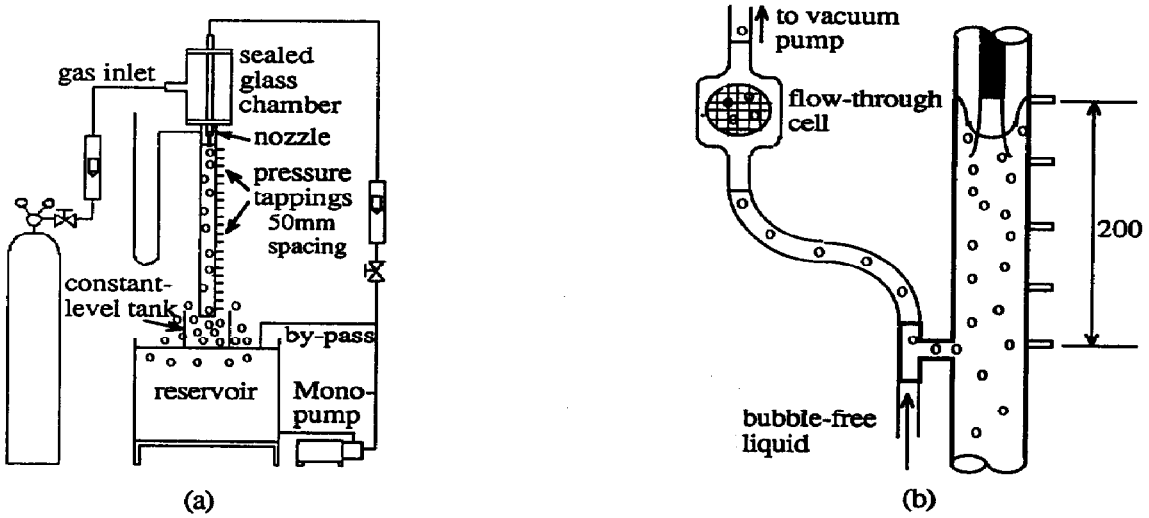

Fig. 2. Experimental apparatus

The jet nozzle was fixed at the top of the column so that the liquid stream was directed along the vertical axis of the column and plunged into the constant level bath below. The overflow from the constant level bath was collected in a much larger vessel from which a Mono pump was used to pump liquid through a rotameter and back to the nozzle. The flow through the nozzle was coarsely adjusted by changing the pulley diameter on the drive shaft for the pump. Fine adjustments were made using the control valve on the by-pass line from the pump outlet and back into the reservoir.

Each nozzle was constructed of brass and consisted of a tapered machined entrance section which fitted neatly inside the nozzle delivery tube giving a smooth transition. The tapered entrance led to the throat of the nozzle which consisted of a straight length of precision-bore brass tubing. Pressure tappings were spaced 50mm apart along the axial length of the column. Another outlet situated 200mm below the top pressure tapping was used to draw the two-phase mixture through the optical flow-through cell as shown in Fig. 2(b). The optical cell was used to photograph the bubbles for determination of the bubble diameter distribution, and it consisted of two parallel glass windows spaced 2mm apart. A 2mm transparent grid was attached to the inside surface of the rear window, and this was used as a length calibration when measuring the bubble size.

Tap water was used as the standard liquid, and Teric 407, a nonionic ethylene oxide derivative produced by Imperial Chemical Industries, was used to control the surface tension of the water. Concentrations of 10, 150 and 1000ppm Teric 407 were used to vary surface tension over the range 65 – 48mN/m. Two aqueous sucrose solutions (16% and 28% by weight sucrose) were also used to vary the viscosity and density of the liquid; the surface tension of each of these solutions was adjusted to 62mN/m by the addition of Teric 407.

Procedure

The gas and liquid flow rates were set at the desired values, allowing the bubble column sufficient time to reach equilibrium. The column was assumed to be at equilibrium when the wall pressure profile became constant with respect to time. At this time the length, L, of the mixing zone was obtained from the wall pressure measurements (see Fig 3).

The two-phase mixture from the mixing zone was drawn through the optical cell with the aid of a jet-ejector pump located upstream of the optical flow-through cell (see Fig. 2b). The rate of bubbles passing between the parallel windows of the optical cell was adjusted in order to minimise the number of overlapping bubbles appearing in the photograph. This was achieved by diluting the two-phase mixture from the mixing zone with the clear liquid prior to it entering the optical cell. Preliminary experiments showed that the measured bubble size was not influenced by the rate at which the bubbly mixture was drawn through the optical cell, and no bubble coalescence was observed. The optical cell and tubing were thoroughly rinsed with 'Nonidet' detergent solution prior to each experiment to minimise bubble-surface interference.

The bubble photographs were taken using a Linhoff Polaroid camera fitted with a 156 mm telephoto lens and extension bellows. The shutter speed was set at 1/250 second with an aperture of f5.6. Backlighting to the flow-through cell was provided by an Olympus flash unit operating at a power ratio of 1/128. The bubble diameter was measured by projecting the negative of the bubble photograph onto a Summographics digitiser pad. The negatives also contained the original 2mm calibration scale, which was used to determine the true size of the bubbles. A minimum of 250 bubbles were measured to determine the diameter distribution for each experiment.

The length of the mixing zone and the resultant bubble diameter distributions were measured for a range of jet and column diameters, jet velocity, gas/liquid volumetric flow ratio, and liquid physical properties. A summary of the conditions for each experiment is given in Table 1.

Table 1: Summary of experimental conditions

Expt No.	D_c (m)	D_j (m)	u_j (m/s)	σ (N/m)	ρ (kg/m^3)	λ_1
1	0.044	0.0071	11.50	0.048[1]	997[2]	0.118
2	0.044	0.0071	11.53	0.054	998	0.116
3	0.044	0.0071	11.50	0.062	998	0.117
4	0.044	0.0048	11.50	0.047	997	0.129
5	0.044	0.0048	11.47	0.053	997	0.129
6	0.044	0.0048	11.50	0.065	997	0.127
7	0.044	0.0024	11.50	0.054	998	0.127
8	0.044	0.0048	11.50	0.064	1061	0.127
9	0.044	0.0048	11.50	0.065	1114	0.131
10	0.044	0.0048	11.47	0.065	999	0.125
11	0.074	0.0071	11.53	0.063	998	0.114
12	0.074	0.0048	15.00	0.065	999	0.126
13	0.074	0.0048	11.47	0.063	999	0.126
14	0.074	0.0048	11.47	0.063	999	0.296
15	0.074	0.0048	11.47	0.063	999	0.645
16	0.074	0.0048	7.80	0.064	999	0.125
17	0.074	0.0024	11.47	0.064	998	0.131
18	0.074	0.0071	11.50	0.061	998	0.114
19	0.074	0.0048	11.50	0.067	999	0.127
20	0.074	0.0024	11.50	0.062	998	0.130
21	0.095	0.0048	11.47	0.063	999	0.125
22	0.095	0.0048	11.50	0.062	998	0.124

[1] Measured using du Nuoy ring method.
[2] Values taken from Weast, R.C. and Astle, M.J. (1980). *CRC Handbook of Chemistry and Physics (60th ed.)*, CRC Press. Florida.

RESULTS AND DISCUSSION

Mixing Zone Length

The axial wall pressure profile was measured as a function of the distance z from the free surface inside the column. The general shape of the pressure profile was similar for each experiment, and a typical set of results is given in Fig. 3, where the absolute pressure P has been normalised with respect to the local atmospheric pressure P_0. In each case it can be seen that there is a distance beyond which the normalised pressure is a linear function of length. This trend indicates a region of relatively constant density and uniform flow, where the increase in pressure corresponds to an increase in the static pressure further down the column – at the base of the column the measured pressure is equal to the atmospheric pressure. In the region of uniform two-phase flow the wall frictional losses increase with increasing superficial liquid velocity as indicated by the increase in slope of the pressure gradient with increasing volumetric flow rate.

Each experimental curve has a section where the pressure profile is not a linear function of distance. This corresponds to a region of higher liquid velocity, due to recirculation of the liquid as a result of the rapid expansion of the confined jet. In the recirculation region the direction of the flow is reversed resulting in a negative dynamic pressure gradient which counterbalances the increase in the hydrostatic pressure, hence the sigmoidal shape of the curve. The mixing zone length was taken as the distance from the free surface inside the column where the pressure profile became linear. The results are listed in Table 2.

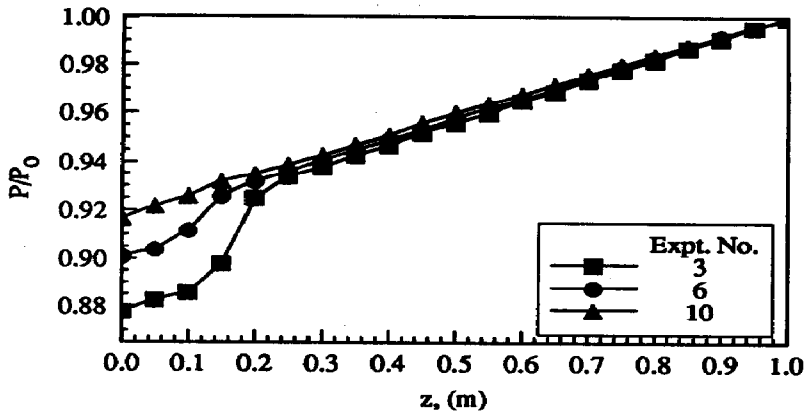

Fig. 3. Axial wall pressure profile

Bubble Diameter Distribution

The form of the bubble diameter distribution generated within the mixing zone was similar for each experiment. A typical cumulative frequency distribution plotted on a log-probability scale produced a linear relationship characteristic of a log-normal distribution. The log-normal distribution was skewed towards the smaller size ranges, possibly as a result of the preferential breakup of the larger bubbles over the more stable smaller bubbles. For many of the experiments the log-probability plots also showed two separate linear regions with different gradients, suggesting that the bubble size distribution was bi-modal. This could possibly be due to the different paths taken by the different size bubbles initially generated in the region close to the point of impact of the plunging liquid jet. The smaller bubbles spend only a short time in the mixing zone before being carried downward by the bulk liquid flow, whereas the larger bubbles are recirculated for a much longer time period before being broken up. The secondary breakup of the larger bubbles could possibly result in another distribution which was different to the initial distribution. If this is the case, then the bi-modal distribution represents (i) the initial distribution of fine bubbles generated by the plunging jet, and (ii) the distribution produced by the gradual breakup of the larger bubbles as they recirculate within the entire mixing zone volume.

Table 2: Summary of results

Expt No.	L (m)	ϵ (10^4kg/ms^3)	pred d_m (μm)	meas d_m (μm)	d_{vs} / d_m
1	0.175	21.40[1]	221[2]	222	0.58
2	0.170	22.20	233	280	0.56
3	0.175	21.40	257	387	0.63
4	0.150	11.50	279	248	0.62
5	0.148	11.60	299	222	0.61
6	0.148	11.70	337	406	0.67
7	0.148	11.70	337	380	0.59
8	0.197	9.31	358	318	0.59
9	0.221	8.67	372	294	0.62
10	0.072	6.06	392	412	0.57
11	0.246	5.63	443	441	0.60
12	0.249	5.53	455	584	0.60
13	0.170	3.61	529	543	0.60
14	0.215	2.86	581	523	0.65
15	0.261	2.35	628	698	0.67
16	0.074	2.62	608	718	0.60
17	0.113	1.37	780	594	0.63
18	0.249	5.52	438	519	0.61
19	0.166	3.73	527	614	0.62
20	0.115	1.34	778	716	0.68
21	0.157	2.38	625	531	0.63
22	0.153	2.46	611	611	0.59

[1] Calculated from eq. (6).
[2] Calculated from eq. (3).

The Sauter mean bubble diameter d_{vs} was calculated from a sample of N bubbles for each experiment, where d_{vs} is defined as

$$d_{vs} = \frac{\sum_{i=1}^{N} (n_i d_i^3)}{\sum_{i=1}^{N} (n_i d_i^2)} , \qquad (7)$$

The results are given in Table 2, and for comparison with other studies they have been normalised with respect to the measured maximum bubble diameter, d_m, which has been taken as the diameter that is greater than 99% of all the diameters in the cumulative frequency distribution. The average value for the bubble diameter ratio d_{vs}/d_m from all of the experiments, was found to be 0.61, with a standard deviation of 0.03. This result is in good agreement with published values, which are in the range 0.60 – 0.62 (Zhang *et al.*, 1985; Calabrese *et al.* 1986; Hesketh *et al.* 1987).

Critical Weber Number

The measured mixing zone length and maximum bubble diameter values listed in Table 2 were used, in conjunction with eqs. (3) and (6), to estimate the critical Weber number. It was found that a critical Weber number of 1.2 gave the best least-squares fit to the data. This value is in agreement with the critical Weber number calculated by Hinze (1955) for bubble breakup in viscous shear flow. Moreover, Sevik and Park (1973) provide some theoretical justification to this value based on the presumption that the bubbles within the mixing zone breakup due to oscillations of the bubble surface which occurs when the frequency of the turbulence corresponds to one of the resonant frequencies of the bubble. However, experimental verification of this breakup mechanism is required.

A comparison of the measured and predicted values using $We_c = 1.2$ is shown in Fig. 4. It can be seen that the predicted maximum bubble diameters were generally within 20% of the measured values.

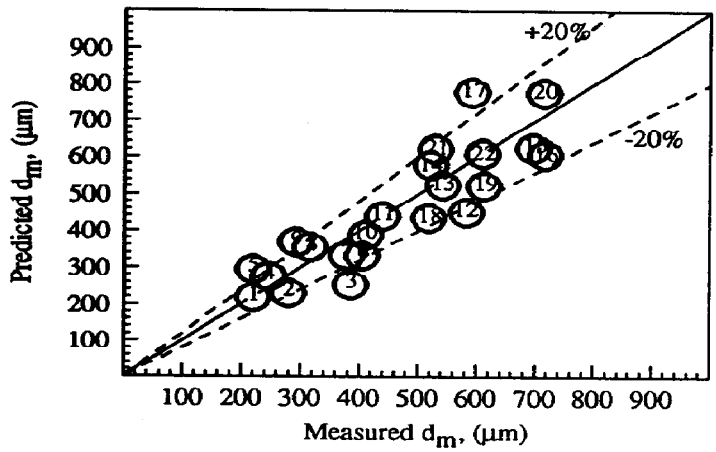

Fig. 4. Comparison between predicted and measured maximum bubble diameter

CONCLUSIONS

The maximum size of bubbles produced within the mixing zone of a plunging liquid jet has been measured and compared with predictions from a simple model. It was found that maximum stable bubble diameter may be predicted simply by determining the length of the mixing zone itself, and assuming the critical Weber number based on the average mechanical energy dissipation rate per unit volume, is equal to 1.2. The predicted maximum bubble diameter has been generally found to agree with measured values to within 20 percent over a wide range of column operating and liquid parameters. It was also found that the bubble size distribution was fitted by a log-probability relationship, and that the ratio of the Sauter mean diameter to the maximium measured bubble size was equal to 0.61, which is in agreement with the results from other experimental studies.

NOTATION

b	jet/column cross-sectional area ratio	
d	bubble diameter	m
d_m	maximum stable bubble diameter	m
d_{vs}	Sauter mean bubble diameter (defined by eq. (7))	m
D_c	column diameter	m
D_j	jet diameter	m
e_s	specific energy dissipation	m^2/s^2
L	length of mixing zone (see Fig. 1b)	m
Q_G	total volumetric gas flow rate rate	m^3/s
Q_L	liquid volumetric flow rate of jet	m^3/s
P	absolute pressure	kg/ms^2
P_0	atmospheric pressure	kg/ms^2
$\overline{u^2}$	average value of the squares of the velocity differences acting over a length scale d	m^2/s^2
u_j	jet velocity at nozzle	m/s
We	Weber number	
z	length down column measured from free surface	m

Greek Symbols

ρ	liquid density	kg/m^3
σ	surface tension	kg/s^2
ε	energy dissipation rate per unit volume	kg/ms^3
λ	gas/liquid volumetric flow ratio	
γ	gas/liquid density ratio	

REFERENCES

Batchelor, G. K. (1951). *Proc. Cambridge Phil. Soc.*, 41, 359.

Calabrese, R. V., T. P. K. Chang and P. T. Dang (1986). Drop breakup in turbulent stirred-tank contactors. Part I: Effect of dispersed-phase viscosity. *A.I.Ch.E. J.*, 32, 657-666.

Cunningham, R.G. (1974). Gas compression with the liquid jet pump. *J. Fluids Eng., Series I*, 3, 203-215.

Evans, G. M. (1990). A study of a plunging jet bubble column. Ph.D. Thesis, University of Newcastle, Australia.

Hesketh, R. P., T. W. Fraser Russell and A. W. Etchells (1987). Bubble size in horizontal pipelines. *A.I.Ch.E. J.*, 33, 663-667.

Hinze, J. O. (1955). Fundamentals of the hydrodynamic mechanism of splitting in dispersion processes. *A.I.Ch.E. J.*, 1, 289-295.

Lewis, D. A.and J. F. Davidson (1982). Bubble splitting in shear flow. *Trans. I. Chem. E.*, 60, 283-291.

Miksis, M., J. M. vanden-Broeck and J. B. Keller (1981). Axisymmetric bubble or drop in a uniform flow. *J. Fluid Mech.*, 108, 89-100.

Ryskin, G. and L. G. Leal (1984). Numerical solution of free-boundary problems in fluid mechanics. Part 3. Bubble deformation in an axisymmetric straining flow. *J. Fluid Mech.*, 148, 37-43.

Sevik, M. and S. H. Park (1973). The splitting of drops and bubbles by turbulent fluid flow. *J. Fluids Eng. Trans. ASME*, 95, 53-60

Zhang, S. H., S. C. Yu, Y. C. Zhou and Y. F. Su (1985). A model for liquid-liquid extraction column performance - the influence of drop size distribution on extraction efficiency. *Can. J. Chem. Eng.*, 63, 212-226.